

RESEARCH

Open Access



Investigating PPT2's role in ovarian cancer prognosis and immunotherapy outcomes

Hui Xu¹, Yan Zhang¹, Zhen Xie¹, Xiao-feng Xie¹, Wen-lan Qiao¹, Miao Wang¹, Bei-bei Zhao¹ and Tian Hua^{1*}

Abstract

Ovarian cancer (OC) remains the primary cause of mortality among gynecological malignancies, and the identification of reliable molecular biomarkers to prognosticate OC outcomes is yet to be achieved. The gene palmitoyl protein thioesterase 2 (PPT2), which has been sparsely studied in OC, was closely associated with metabolism. This study aimed to determine the association between PPT2 expression, prognosis, immune infiltration, and potential molecular mechanisms in OC. We obtained the RNA-seq and clinical data from The Cancer Genome Atlas (TCGA), The Genotype-Tissue Expression (GTEx) and Gene Expression Omnibus (GEO) databases, then Kaplan-Meier analysis, univariate Cox regression, multivariate Cox regression, nomogram, and calibration were conducted to assess and verify the role of PPT2. Gene set enrichment analysis (GSEA) was used to figure out the closely correlated pathways with PPT2. Overexpression experiment was performed to explore the function of PPT2. Our findings showed that PPT2 mRNA expression was apparent down-regulation in OC tissue compared to normal ovarian tissues in TCGA, GTEx datasets, and GEO datasets. This differential expression was also confirmed in our in-house datasets at both the mRNA and protein levels. Decreased PPT2 expression correlated with lower survival rates in TCGA, several GEO datasets, and our in-house datasets. Multivariate analysis revealed that PPT2 was an independent factor in predicting better outcomes for OC patients in TCGA and GEO. A negative correlation was revealed between immune infiltration and PPT2 expression through Single-sample GSEA (ssGSEA). Additionally, PPT2 was negatively correlated with an up-regulated immune score, stromal score, and estimate score, suggesting that patients with low PPT2 expression might benefit more from immunotherapy. Numerous chemical agents showed lower IC50 in patients with high PPT2 expression. In single-cell RNA sequencing (scRNA-seq) analysis of several OC datasets, we found PPT2 was mainly expressed in endothelial cells. Furthermore, we found that PPT2 inhibited OC cell proliferation in vitro. Our results demonstrated that PPT2 was considered a favorable prognostic biomarker for OC and may be vital in predicting response to immunotherapy and chemotherapy. Further research was needed to fully understand the relationship between PPT2 and immunotherapy efficacy in OC patients.

Keywords PPT2, Ovarian cancer, Prognosis, Immunotherapy response, Tumor microenvironment

*Correspondence:

Tian Hua

huatian1982@163.com

¹Department of Gynecology, Affiliated Xingtai People Hospital of Hebei Medical University, 16 Hongxing Road, Xingtai, Hebei 054001, China



© The Author(s) 2024. **Open Access** This article is licensed under a Creative Commons Attribution-NonCommercial-NoDerivatives 4.0 International License, which permits any non-commercial use, sharing, distribution and reproduction in any medium or format, as long as you give appropriate credit to the original author(s) and the source, provide a link to the Creative Commons licence, and indicate if you modified the licensed material. You do not have permission under this licence to share adapted material derived from this article or parts of it. The images or other third party material in this article are included in the article's Creative Commons licence, unless indicated otherwise in a credit line to the material. If material is not included in the article's Creative Commons licence and your intended use is not permitted by statutory regulation or exceeds the permitted use, you will need to obtain permission directly from the copyright holder. To view a copy of this licence, visit <http://creativecommons.org/licenses/by-nc-nd/4.0/>.

Introduction

Among gynecological cancers, ovarian cancer (OC) has ranked as the second most frequent cause of death [1]. GLOBOCAN cancer statistics for the year 2020 showed that OC was the eighth most common and fatal cancer diagnosed among women worldwide [2, 3]. Approximately 70% of OC patients were diagnosed with peritoneal or distant metastasis at the time of diagnosis due to the lack of specific symptoms, making it challenging to identify the disease early and could lead to poorer patient outcomes [4]. Combined chemotherapy with platinum-based derivatives and taxanes was the first-line treatment for advanced OC patients following primary surgery. About 80% of patients showed an excellent response to initial chemotherapy. However, the majority of patients within 24 months would suffer a relapse of the platinum-resistant tumors. The 5-year overall survival (OS) rate of patients diagnosed with advanced-stage OC has persisted at a dishearteningly low range of 25–35% for decades [5]. In recent years, there have been significant strides in the treatment of OC. Poly-ADP ribose polymerase (PARP) inhibitors, like olaparib, and antiangiogenic agents, such as bevacizumab, appeared to have the potential to postpone the recurrence of the ailment [6]. However, the vast majority of patients still suffered a tumor recurrence and eventually developed platinum resistance. Therefore, it was necessary to explore effective biomarkers for the prediction of prognosis and response to new treatment strategies.

Palmitoyl protein thioesterase (PPT) was a lysosomal enzyme that mainly served as the thioester link between fatty acids and cysteine in lipid-modified proteins and removed long-chain fatty acids from cysteine residues in proteins [7]. PPT1 and PPT2 were the two types of PPT [8]. PPT2 encoded a member of the palmitoyl-protein thioesterase family. Both two PPTs had a significant impact on lysosomal thioester catabolism [9]. PPT1 has been observed to be expressed in various types of cancer, such as liver, thyroid, and gastric cancers [10]. It has been demonstrated that increased expression of PPT1 in hepatocellular carcinoma is linked with a reduced OS [11]. At present, PPT2 has rarely been studied in cancer. It was still uncertain whether PPT2 played a comparable role in tumorigenesis as PPT1. According to a recent study, PPT2 was found to be downregulated in clear cell renal cell carcinoma when compared to normal control tissues. Overexpression of PPT2 repressed the clear cell renal cell carcinoma (ccRCC) progression by reducing epithelial-to-mesenchymal transition (EMT), the reduced expression of PPT2 could potentially serve as a novel diagnostic and prognostic biomarker, as well as a target for therapeutic interventions [12, 13]. However, there has been no report about the role of PPT2 in OC and its effect on prognosis yet.

In this study, we explored the potential prognostic value of PPT2 in OC for the first time. Real time-quantitative PCR (RT-qPCR) and immunohistochemistry (IHC) analyses were conducted in an in-house independent OC cohort. Concerning the correlation with clinical characteristics, patient prognosis, drug sensitivity, levels of immune infiltration, and the biological function of PPT2 were investigated based on the bioinformatics tools and datasets of TCGA, GTEx, GEO, GSEA, STRING, CytoHubba plug-in, and TIMER. In addition, a nomogram based on PPT2 expression and clinical factors was developed for OC patients to predict patient outcomes. We also found PPT2 mainly expressed in the endothelial cells by single-cell RNA sequencing (scRNA-seq) analysis in the Tumor Immune Single-cell Hub 2 (TISCH2) database. Through clinicopathologic and survival analysis, as well as in vitro studies of OC cells, we demonstrated that PPT2 may be a valuable novel therapeutic agent against OC.

Materials and methods

Data collection

PPT2 expression profiles in OC from the GTEx project and TCGA dataset, and all the information we downloaded was from the UCSC Xena (<https://xena.ucsc.edu/platform>) [14]. The pan-cancer expression differential and survival analysis of PPT2 was done by R package “UCSCXenaShiny” [15]. We obtained external validation datasets of PPT2 expression data from GSE27651, GSE29450, GSE40595, and GSE51088. We obtained external validation datasets of PPT2 survival and corresponding clinical information of OC patients from GSE23554, GSE26712, GSE32063, GSE51088, GSE63885, and GSE140082.

Nomogram construction

We downloaded the clinical information of OC patients (with complete details of age, stage, grade, tumor residual size, and PPT2 mRNA expression) in this study from the UCSC Xena (<https://xena.ucsc.edu/platform>). The nomogram and calibration curve were plotted by R package “regplot”. Nomogram could predict patients’ prognosis by integrating different prognostic factors to produce personalized clinical event probability. We used the calibration curves to evaluate nomogram accuracy.

GSEA analysis

R package “clusterProfiler” was used to analyze the significantly enriched HALLMARK between the high and low expression of PPT2 [16, 17]. The pathway metric of $p < 0.05$, $FDR < 0.05$ and $|NES| > 1$.

Immune infiltration analysis

The ESTIMATE algorithm (R package “ESTIMATE”) was conducted to extract scores of stromalScore, immuneScore, and estimateScore [18]. ssGSEA was employed to quantify immune cells and immune function (R package “GSVA”, “GSEABase”). With a comprehensive assessment of the immune infiltration website TIMER database [19] (<http://timer.cistrome.org/>) and assessed the relationship between PPT2 expression and immune infiltration score using the spearman’s correlation analysis.

Drug sensitivity assessment

The half-maximal inhibitory concentration (IC₅₀) of chemotherapy drugs from the Genomics of Drug Sensitivity in Cancer (GDSC) (<https://www.cancerrxgene.org/>) [20] was retrieved to analyze in the TCGA dataset (R package “pRRophetic”) [21].

Protein interaction network (PPI)

The LinkedOmics database (<http://www.linkedomics.org/login.php>) [22] was employed for PPT2 co-expression analysis based on Spearman’s correlation coefficients. The heatmap was conducted to plot the results. STRING (v11.5, <http://string-db.org/>) [23] was an online tool to conduct the protein-protein interaction network functional enrichment analysis, we selected the organism as human specimens, and input the PPT2 positively related genes (correlation coefficient > 0.3, $p < 0.05$), then a cutoff value of 0.4 for minimum interaction score was set to obtain biological functions, with disconnected nodes hidden from network. Then, Cytoscape 3.9.0 [24] was used to visualize the interaction network of these proteins, and hub genes (filtering degree ≥ 10) were also acquired using the CytoHubba plug-in.

Clinical specimens

A total of 45 freshly frozen OC tissue samples were collected in the first surgery from Aug. 2018 to Aug. 2019 at Affiliated Xingtai People Hospital of Hebei Medical University. In total, nine normal ovary tissues were collected from patients who received adnexectomy due to the gynecological benign diseases from Aug. 2018 to Aug. 2019. The 45 OC patients were followed up regularly for 3 years after the initial surgery. The survival status of the patients was evaluated by PFS and OS. The Affiliated Xingtai People Hospital of Hebei Medical University Ethics Committee reviewed and approved our study (2018 [07]). Written informed consent was provided by all patients.

RT-qPCR analysis

TRIzol reagent (Generay Biotech, China) was used to extract total RNA based on the manufacturer’s protocol. Using Revert-Aid First Strand cDNA Synthesis Kit

(Thermo Scientific, U.S.A.), 500ng total RNA was used to synthesize cDNA. With β -actin as a housekeeping gene and primers bought from Sangon Biotech Co. Ltd. (Shanghai, China), QuantiNova TMSYBR® Green PCR Kit (Qiagen, Hilden, Germany) was applied for RT-qPCR. Custom primers for PPT2 (F: GGAAGAGCCCCATGCACCACGA TT, R: GAAGAGCCCCATGCACCACGA) and β -actin (F: GTGGCCGAGGACTTTGATTG, R: CCTGTAACAACGCATCTCATATT) were acquired from Sangon Biotech Co. Ltd. (Shanghai, China).

Immunohistochemistry (IHC) staining

Nineteen tissue samples from 45 OC patients and nine normal ovary tissues were obtained, and IHC staining was performed for PPT2 using the PPT2 antibody (abs151365, 1:200, Absin, Bioscience Inc., Shanghai, China). Nuclear staining without cytoplasmic staining was considered positive. Specifically, staining intensity and percentage of the positive staining area of the IHC results were set as judgment criteria. The predicted location for PPT2 was considered in intracellular. Specifically, the definition of negative, weak, moderate, and strong staining was no nuclear staining of cells, nuclear staining of < 25%, 25-75%, and > 75%, respectively.

Cell culture

Human OC cell lines A2780, OVCAR3, OVCAR8 and OVCA433 cell lines used in this study were purchased from the American Type Culture Collection (ATCC, Manassas, VA, USA). The HEK293T cell line was obtained from the Chinese Academy of Sciences (Shanghai, China). Cell lines were authenticated by short tandem repeat (SRT) profiling.

Establishment of stable cell lines

The full-length cDNA of PPT2 was amplified and cloned into the PLVX-puro lentiviral vector, the lentiviral expression plasmids were co-transfected with packaging plasmids (pMD2G and psPAX2) into HEK293T cells using lipofectamine 3000 (Invitrogen, CA, USA). The supernatants were harvested and filtered through 0.45 μ m filters (FPV403030, JET BIOFIL, Guangzhou, China) after transfection for 48 h. lentiviral infection was performed by incubating cells with the virus-containing medium with polybrene for 24 h. Stable cells were then selected with 2 μ g/ml puromycin.

siRNA transient transfection

Synthetic siRNA oligonucleotides targeting PPT2 were designed and synthesized by RiboBio (Guangzhou, China). Transfection of PPT2 siRNAs was performed using lipofectamine 3000 (Invitrogen, CA, USA) according to the manufacturer’s instructions.

Western blot analysis

Cells were collected and lysed with RIPA buffer. Proteins were subject to SDS-PAGE, and transferred to the PVDF membrane (Millipore, Billerica, MA, USA). Following blocking with Bovine Serum Albumin (Beyotime, China), the blots were incubated sequentially with primary and secondary antibodies, and then visualized using an ECL detection kit (Millipore). The anti-PPT2 and anti-β-actin antibodies were purchased from Proteintech (Wuhan, Hubei, China).

Cell proliferation, colony formation

Cell proliferation was measured with Cell Counting Kit-8 (CCK-8) (Dojindo, Japan). OC cells were plated at 1×10^3 cells/well in the 96-well plates, and the absorbance of the samples was evaluated at 450 nm every 24 h for 5 consecutive days. For the colony formation assay, OC cells were seeded at 1×10^3 cells/well in 6-well plates and cultured under normal growth conditions for nearly 14 days. Colony formation was determined by counting the number of stained colonies by crystal violet.

Transwell invasion assay

For invasion assay was performed using transwell chamber inserts in a 24-well plate, 5×10^4 cells were seeded in 100 μL of serum-free medium were added to the upper

chamber coated with Matrigel (Corning, USA), while the lower chambers were filled with the normal culture medium. The cells were cultured for 36 h. Then the cells on the lower surface were fixed with methanol and stained with crystal violet. The number of migrating cells was counted in randomly selected fields with a microscope.

Statistical analysis

R software v3.6.3 was applied for all statistical analyses. The Chi-square test or Fisher’s exact test was applied for analyzing qualitative variables. Quantitative variables analyses were performed using the Wilcoxon rank-sum test. The Kaplan-Meier survival analysis was conducted by log-rank test. If not specified above, $p < 0.05$ was statistically significant.

Results

In the schematic diagram of the study, the wet and dry laboratory experiments were shown in Fig. 1.

PPT2 is down-regulated in OC tissues

The archived information of 45 OC patients was obtained from the Affiliated Xingtai People Hospital of Hebei Medical University. The median age of the patients was 57 years (ranging from 24 to 77). Concerning the

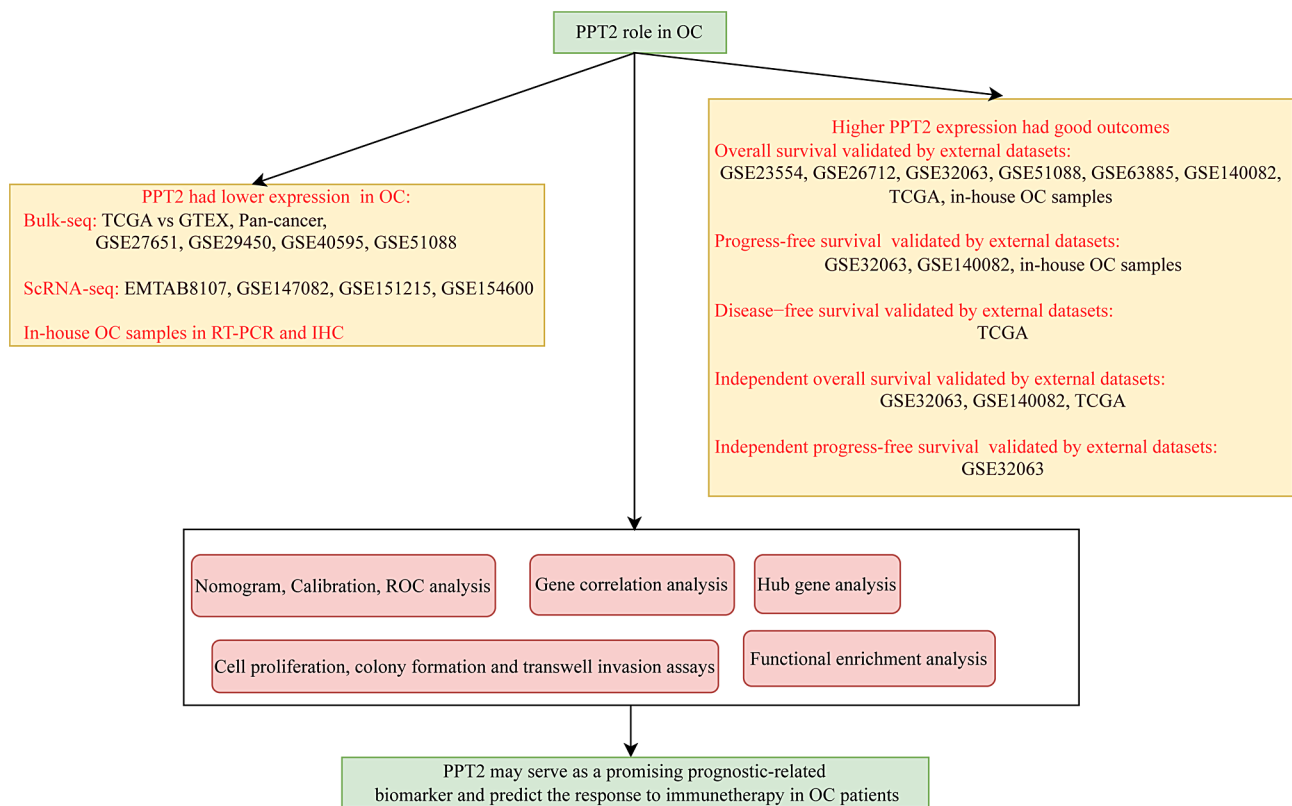


Fig. 1 Schematic diagram representation of the study design

histology, 27 (60.0%) out of the 45 patients were diagnosed with serous adenocarcinoma, 10 (22.2%) with endometrioid carcinoma, 4 (8.9%) with clear cell carcinoma, and 4 (8.9%) with mixed type. According to FIGO (International Federation of Gynecology and Obstetrics) staging, 10 cases (22.2%) had stage I-II OC, and 35 cases (77.8%) were in stage III-IV. Detailed information was shown in Table 1. The normal ovary tissues of 9 patients who underwent the adnexectomy because of benign gynecological diseases were collected. The median age was 51 years old (ranging from 46 to 73). They had never had a diagnosis of cancer before.

RT-qPCR was performed to detect PPT2 mRNA expression in 45 OC tissues and 9 normal ovary tissues. Compared to PPT2 mRNA expression in the normal ovary tissues, an apparent down-regulation was observed in OC tissues (Fig. 2A). Additionally, the PPT2 mRNA expressions from the TCGA and the GTEx were compared, and the PPT2 expression was high in normal samples (Fig. 2B). Additionally, we also found that PPT2 was highly expressed in normal samples in GEO datasets, GSE27651, GSE29450, GSE40995, and GSE51088, respectively. (Figs. 2C-F). We also separately analyzed the PPT2 expression profile in pan-cancer from the TCGA and GTEx datasets. PPT2 exhibited a notable decrease in expression across various types of tumors, such as cervical cancer (CESC), kidney chromophobe (KICH), and lung adenocarcinoma (LUAD). On the contrary, the higher expression of PPT2 in tumor was observed in lymphoid neoplasm diffuse large B-cell lymphoma (DLBC), glioblastoma multiforme (GBM), and skin cutaneous melanoma (SKCM) (Fig. 2G), which indicated the

different roles of PPT2 in pan-cancer. In contrast with normal ovary tissues, the expression of PPT2 protein in the OC tissues was significantly weaker by IHC (Fig. 2H; Table 2). The expression status of PPT2 in the OC related scRNA-seq datasets was explored on the TISCH2 website. The results revealed a conspicuous enrichment of PPT2 expression in the endothelial cells other than malignant cells in EMTAB8107, GSE147082, GSE151214, GSE154600 (Fig. 3). Therefore, we surmised that PPT2 was down-regulated in tumor and might serve as one of the tumor suppressors in OC.

Low PPT2 expression significantly correlated with the unfavorable prognosis in OC

To investigate the prognostic implications of PPT2 in OC, the Kaplan-Meier analysis was conducted in an in-house independent cohort of 45 OC patients. The patients were divided into two groups based on the median value of PPT2 mRNA expression. In contrast with those patients with high PPT2 expression, the low PPT2 expression patients showed significantly shorter OS (Fig. 4A), and shorter progression-free survival (PFS) (Fig. 4B). We validated the OS in the datasets GSE23554, GSE26712, GSE32063, GSE51088, GSE63885, GSE140082 and TCGA, and low PPT2 expression were all observed to be significantly related to poorer OS in OC (Fig. 4C). We then validated the PFS in the datasets GSE32063, GSE140082, and low PPT2 expression were all observed to be significantly related to poorer PFS in OC (Fig. 4D). We also validated the disease-free survival (DSS) in TCGA, and low PPT2 expression was observed to be significantly related to poorer DSS in OC (Fig. 4E). In TCGA pan-cancer OS analysis, PPT2 was proved to be protective in OC, kidney renal clear cell carcinoma (KIRC), pancreatic adenocarcinoma (PAAD), and thymoma (THYM). PPT2 was proved to be risky in bladder urothelial carcinoma (BLCA), lung adenocarcinoma (LUAD), and thyroid carcinoma (THCA) (Fig. 4F). The above results proved that the PPT2 expression level was close to clinical outcome of many cancers, especially in OC.

Nomogram estimation

To detect whether PPT2 took an independent prognostic association part in OC patients, a multivariable survival analysis was performed with PPT2 expression combined with clinical features datasets GSE140082, TCGA, and GSE32063, suggesting that PPT2 expression may be a novel independent OS biomarker for OC patients (Fig. 5A-C). We also found that PPT2 expression may be a novel independent PFS biomarker for OC patients in dataset GSE32063 (Fig. 5D). Then multivariate Cox regression analysis was used to build a gene-clinical nomogram furtherly, including PPT2 expression and

Table 1 The clinicopathological characteristics of OC patients

Characters	Histology/Stage	Patients (n)	Median	Percentage/Range
Age		45	57.5 years	24–77 years
Histology	Serous	27		60.0%
	Endometrioid	10		22.2%
	Clear cell	4		8.9%
	Mixed type	4		8.9%
FIGO stage	I-II	10		22.2%
	III-IV	35		77.8%
Histological grade	G1	9		20.0%
	G2	11		24.4%
	G3	25		55.6%
Tumor residual size	0 cm	17		37.8%
	≤ 1 cm	21		46.7%
	> 1 cm	7		15.5%
Follow-up time		45	27 months	14–36 months

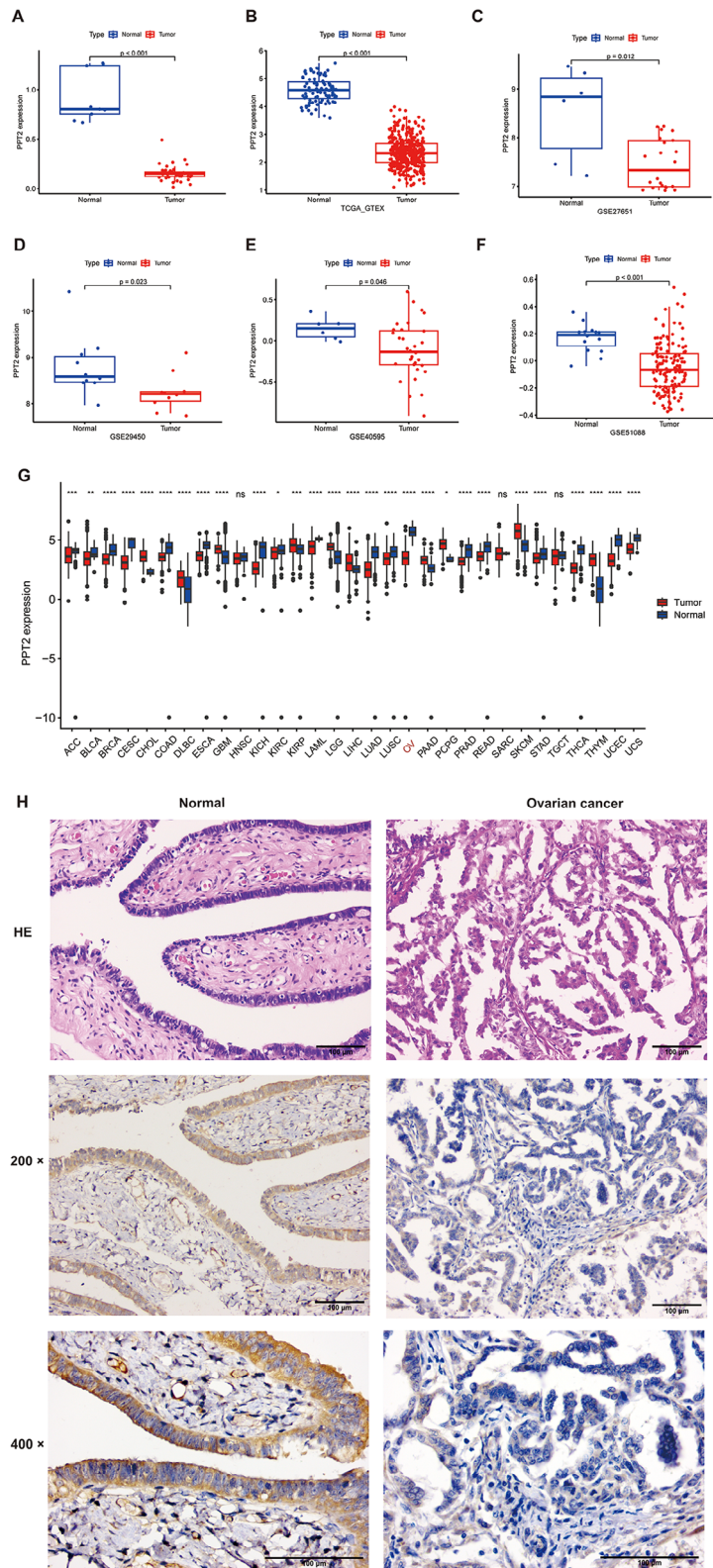


Fig. 2 The expression of PPT2 in OC. **(A)** The comparison of PPT2 mRNA expression in 45 OC tissues and 9 normal ovary tissues. **(B)** The comparison of the PPT2 mRNA expression between the OC tissues and normal tissues in the TCGA and GTEx datasets. **(C-F)** The comparison of PPT2 protein in OC tissues and normal ovary tissues in datasets GSE27651, GSE29450, GSE40995, and GSE51088, respectively. **(G)** The comparison of PPT2 expression in pan-cancer tissues and normal tissues. * $p < 0.05$, ** $p < 0.01$, and *** $p < 0.001$. **(H)** The IHC of normal and OC tissues

Table 2 The PPT2 protein levels in the OC and normal ovary tissues

PPT2 expression	OC tissues N (%)	Normal ovary tissues N (%)	P
Negative	7	0	0.003
Weak	10	2	
Moderate	2	4	
Strong	0	3	

multiple clinical factors, which could visually and accurately predict the survival of patients at 1, 3 and 5 years based on PPT2 expression and clinical information (Fig. 5E). The calibration plots for the nomogram model indicated that the observed rate was well-matched with the predicted values by the nomogram (Fig. 5F). The (Area under the curve) AUCs of 1-year (AUC=0.711), 3-year (AUC=0.643), and 5-year (AUC=0.647) ROC curves predicted by the nomogram score suggesting the efficiency of nomogram in predicting prognosis for OC to a certain extent.

Functional analysis of PPT2 in OC

To explore the biological effects associated with PPT2 in OC, functional enrichment analysis between high and low expression of PPT2 was conducted using GSEA analysis across the entire set. The highly related HALLMARK pathways in the low expression of the PPT2 subgroup were HALLMARK EPITHELIAL MESENCHYMAL TRANSITION, HALLMARK IL6 JAK STAT3 SIGNALING, HALLMARK KRAS SIGNALING UP (Fig. 6A). To deeply understand the biological roles of PPT2 in OC, we analyzed the gene expression correlation with all other genes, the positively and negatively correlated significant genes were presented (Fig. 6B-C). According to the method MCC in CytoHubba, we found ten hub genes (VPS52, RGL2, SLC39A7, PFDN6, COL11A2, RXRB, ZBTB9, RING1, WDR46, and CUTA) from all the interacted genes (Fig. 6D).

Assessment of the immuno-/chemotherapeutic response in the risk subtypes for OC patients

We calculated the infiltrating scores of 16 types of immune cells and 13 immune-related functions or pathways to investigate the correlation between the PPT2 expression and immune infiltration. The significantly different abundances of the immune cells between the high and low PPT2 expression subgroups were observed, including B cells, NK cells, Th1 cells. What's more, the immune-related functions, such as APC-co-stimulation, inflammation-promoting, and cytolytic activity, showed clear differences between the high and low PPT2 expression groups. (Fig. 7A). Besides, patients with low PPT2 expression had a higher estimate score, immune score, and stromal score, implying an obviously different tumor

immune infiltration level in different expressions of PPT2 (Fig. 7B). Multiple immune cells also exhibited negative relations to the expression level of PPT2 via different algorithms, such as TIMER, EPIC, and XCELL (Fig. 7C-D). Above all, we surmised that OC patients with low PPT2 expression might be more suitable for immunotherapy, which may provide laboratory evidence for individual therapies. The IC50 values of the low PPT2 and high PPT2 groups were calculated based on the GDSC data, we found that the IC50 values of the A-770,041, CGP-60,474, Dasatinib, DMOG, Erlotinib and JW-7-52-1 were lower in the low PPT2 group (Fig. 8). The above results demonstrated that the poor prognosis of low high PPT2 patients might be more sensitive to the immunotherapy and chemotherapy.

PPT2 reduced proliferation and invasion of OC cells

In order to demonstrate the functional significance of PPT2 in OC, the stable PPT2-overexpressed OVCAR3 and A2780 cell lines were generated, we validated the PPT2-overexpressed in mRNA and protein levels (Fig. 9A-B, Figure S1). As shown in the results, overexpression of PPT2 significantly inhibited the proliferation of OVCAR3 and A2780 cells lines (Fig. 9C, D, F, G). At the cellular level, transwell assays showed that the PPT2 overexpression group could significantly inhibit the invasion of OVCAR3 and A2780 cells lines (Fig. 9E, H). Furthermore, we knocked down the expression of the PPT2 in OVCAR8 and OVCA433 cells, we validated the PPT2 knockdown efficiency in mRNA and protein levels (Fig. 10A-B, Figure S1). Decreased expression of PPT2 significantly promoted the proliferation of OVCAR8 and OVCA433 cells lines (Fig. 10C, D, F, G). Transwell assays showed that the decreased expression of PPT2 significantly promoted the invasion of OVCAR8 and OVCA433 cells lines (Fig. 10E, H). These results suggested that PPT2 could inhibit the proliferation and metastasis of OC cells in vitro.

Discussion

It has been identified that four distinct acyl protein thioesterases possessed the catalytic ability to facilitate depalmitoylation, with PPT2 being among their ranks [25]. For several biological processes, enzymes that regulated protein palmitoylation were critical. The limited space between two parallel loops (beta3-alphaA and beta8-alphaF) located immediately above the lipid-binding groove in PPT2 restricted the binding of fatty acids with bulky head groups, and this binding groove was significantly larger in PPT1, revealing the basis for divergent substrate specificities of the two lysosomal thioesterases, PPT1 and PPT2 [26]. PPT1 promoted tumor growth and was the molecular target of chloroquine derivatives in cancer [10]. GNS561, a clinical-stage PPT1 inhibitor, was

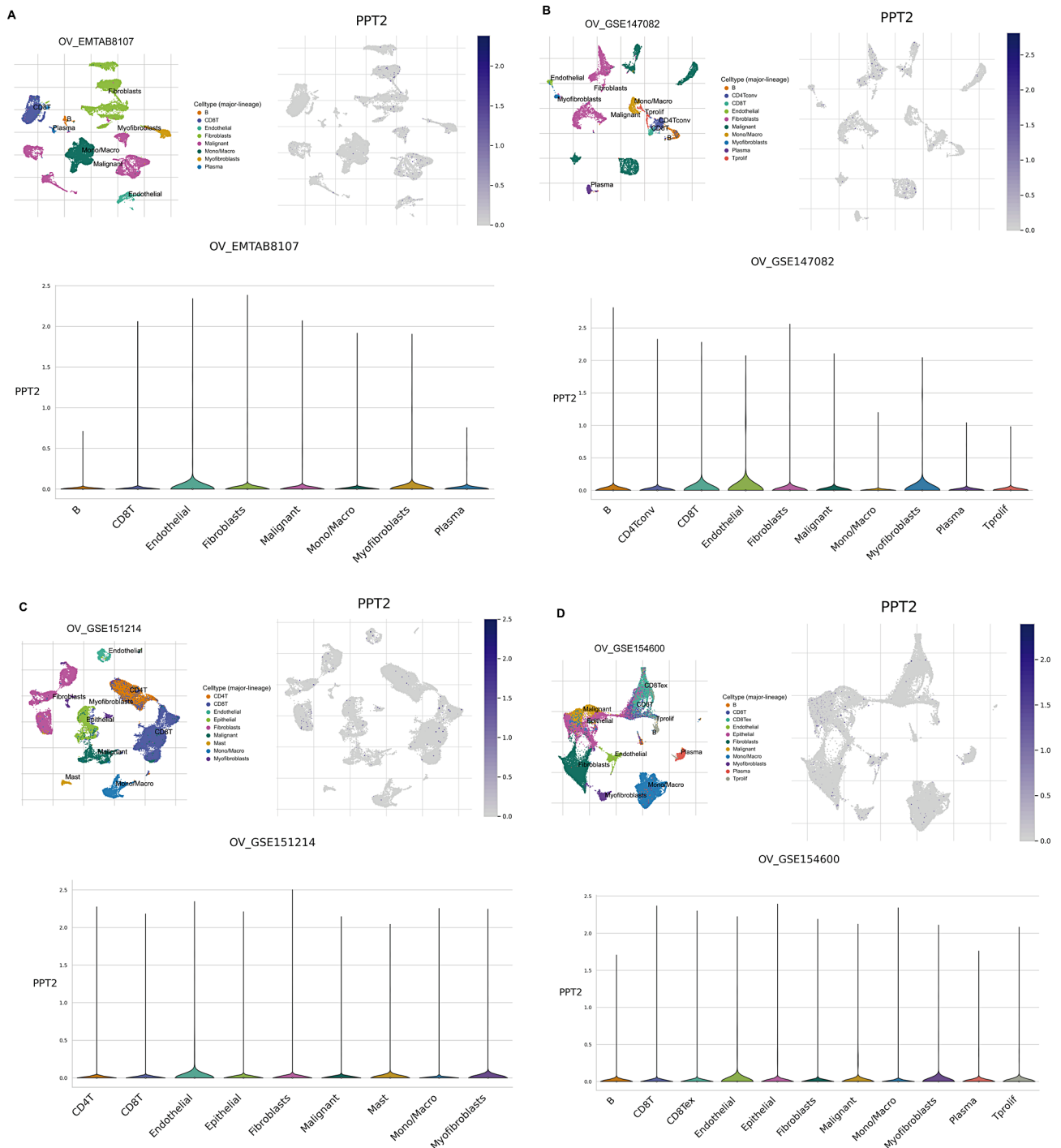


Fig. 3 The expression status of PPT2 in OC single-cell database. (A-D) The expression of PPT2 was lower in malignant cell type in OC datasets EMTAB8107, GSE147082, GSE151214, and GSE154600

efficient against hepatocellular carcinoma via modulation of lysosomal functions [27, 28]. High PPT1 expression predicted poor clinical outcome and PPT1 inhibitor DC661 enhanced sorafenib sensitivity in hepatocellular carcinoma [11]. A lack of PPT1 (due to gene mutations) caused the progressive death of cortical neurons and was responsible for infantile neural ceroid lipofuscinosis

(INCL), a severe neurodegenerative disorder in children [29]. PPT1 promoted the proliferation of hepatocellular carcinoma cells in vitro and quantitative proteomics and bioinformatics analysis confirmed that PPT1 acts by affecting the metabolism, localization, and function of various macromolecular proteins [30]. PPT1 reduction contributed to erianin-induced growth inhibition

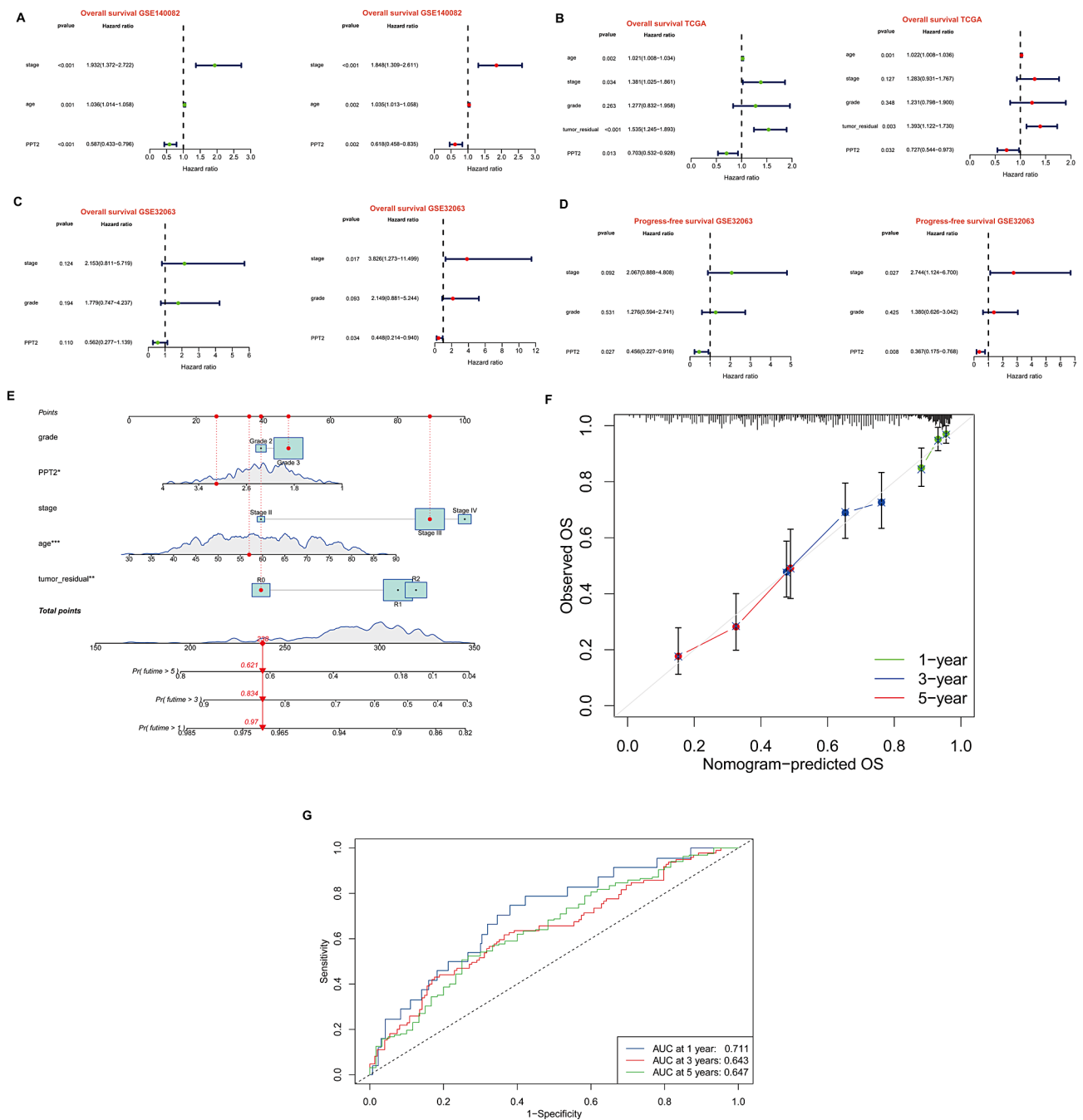


Fig. 5 PPT2 served as an independent prognostic factor in OC (A-C) Univariate and multivariate Cox regression analysis for OS in datasets GSE140082, TCGA, and GSE32063. (D) Univariate and multivariate Cox regression analysis for PFS in dataset GSE32063. (E) Nomogram predicting 1-year, 3-year and 5-year survival. * $p < 0.05$, ** $p < 0.01$, and *** $p < 0.001$. (F) Calibration curves for 1-year, 3-year and 5-year survival probability. (G) The 1-year (0.711), 3-year (0.643), 5-year (0.647) ROC curves predicted by the nomogram score

in oral squamous carcinoma cells [31]. PPT1 inhibition enhanced the antitumor activity of anti-PD-1 antibody in melanoma [32]. DQ661 was a novel dimeric quinacrine that affected multiple lysosomal functions (autophagy and macropinocytosis) and mTORC1 (mechanistic target of rapamycin) activity by specifically targeting PPT1 [28]. Inhibition of PPT1 using ezurpimtrostat decreased

the liver tumor burden in a mouse model of hepatocellular carcinoma by inducing the penetration of lymphocytes into tumors when combined with anti-PD-1 [33]. The effect of PPT2 downregulation on STING palmitoylation may be related to acyl-CoA metabolism in gene therapy [34]. PPT2 transferred the phosphopantetheinyl group of coenzyme A to the acyl carrier protein Acp1

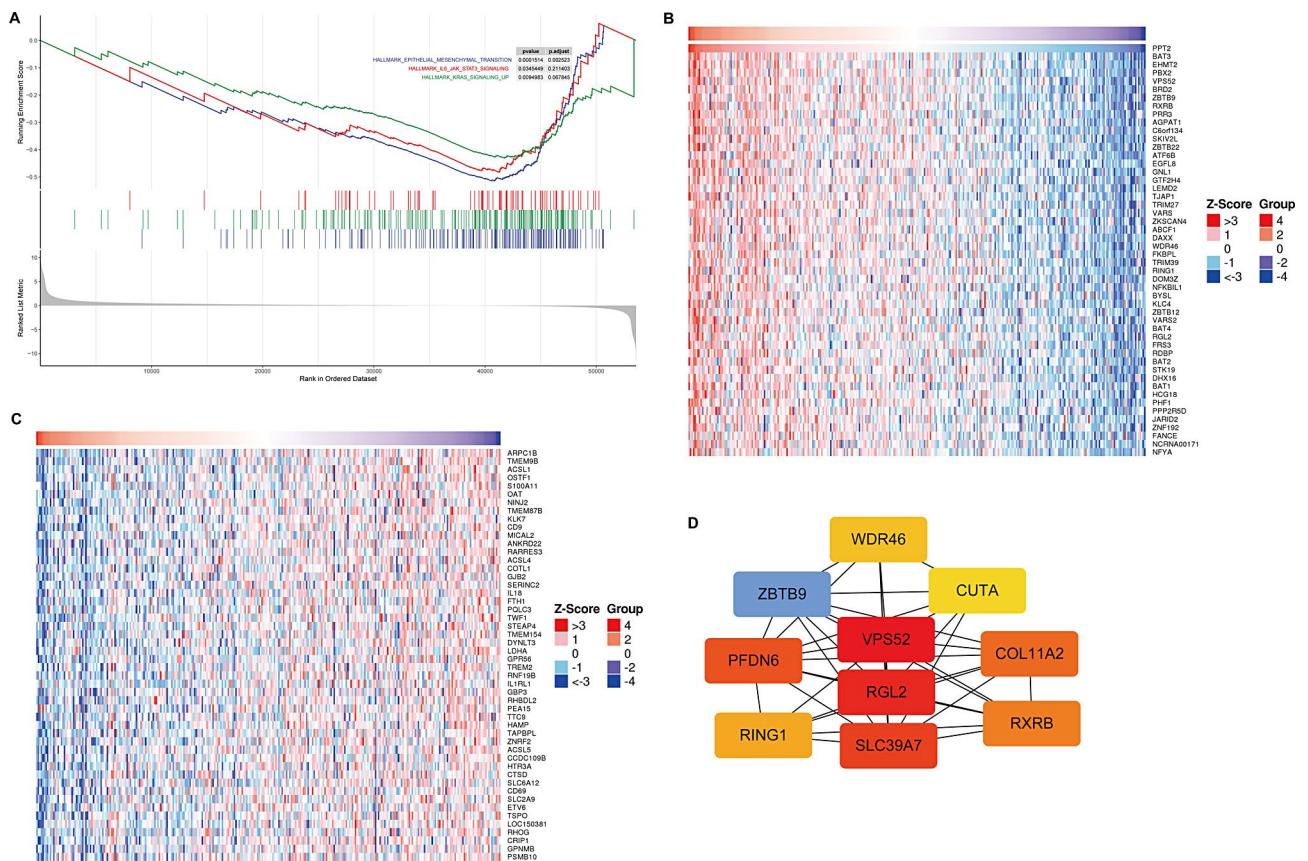


Fig. 6 Functional Analysis of PPT2 in OC. **(A)** Highly enriched hallmark pathways in the low PPT2 expression group (all $p < 0.05$, $FDR < 0.25$, $|NES| > 1$). **(B)** The global PPT2 highly correlated genes identified by Spearman's test in the TCGA cohort (LinkedOmics). **(C)** The top 50 positively and 50 negatively correlated significant genes of PPT2 were presented in the heatmap. **(D)** The hub genes (VPS52, RGL2, SLC39A7, PFDN6, COL11A2, RXRB, ZBTB9, RING1, WDR46, and CUTA) associated with PPT2 were identified in OC by CytoHubb

in mitochondria for the synthesis of lipoic acid that was essential for fungal respiration, so making PPT2 an ideal target for antifungal drugs [35, 36]. PPT2 deficiency in mice caused an unusual form of neuronal ceroid lipofuscinosis with striking visceral manifestations [37]. Overexpression of PPT2 repressed the proliferation, migration and invasion of ccRCC cells in vitro progression by reducing EMT [12]. PPT2 belonged to a differentially methylated region related to survival in oropharyngeal cancer [38]. The comprehensive review of previous studies on PPT revealed that research on PPT1 was extensive, encompassing cellular functions, molecular pathways, and even clinical pharmacology. In contrast, investigations into PPT2 were comparatively limited. This disparity underscored the necessity for further exploration of PPT2 and was compelling reason to believe that PPT2 also held significant potential for clinical research.

The present study investigated the possible role of PPT2 in OC. First, it showed that the PPT2 expression was markedly lower in OC tissues compared with normal ovary tissue in both mRNA and protein levels in our in-house dataset. Consistent results were observed

in the TCGA, GTEx, and other GEO datasets. We also presented the pan-cancer differential expression of PPT2, PPT2 showed a significant differential expression in many cancer types. However, another essential protein thioesterase, PPT1, was significantly up-regulated in OC tissue compared with normal ovary tissue in TCGA and GTEx datasets (Figure S2). The thioester bonds in S-fatty acylated proteins, linking fatty acids to cysteine residues were hydrolyzed by PPT1. PPT2 like PPT1 targeted lysosomes through the mannose 6-phosphate receptor pathway and was extremely active against palmitoylated model substrates such as palmitoyl CoA [39]. PPT2 could not rescue the neural inclusion phenotype connected with the loss of PPT1 even though they were highly similar, and that was what suggested distinct functions and substrates for these two thioesterases [26]. Therefore, PPT1 and PPT2 may play different roles in tumor development.

Subsequently, regarding the expression of PPT2 and clinical outcomes, we used multiple datasets to analyze the relationship between them. The results presented here concluded that patients with low PPT2 expression had a significantly poorer clinical outcome in OC from

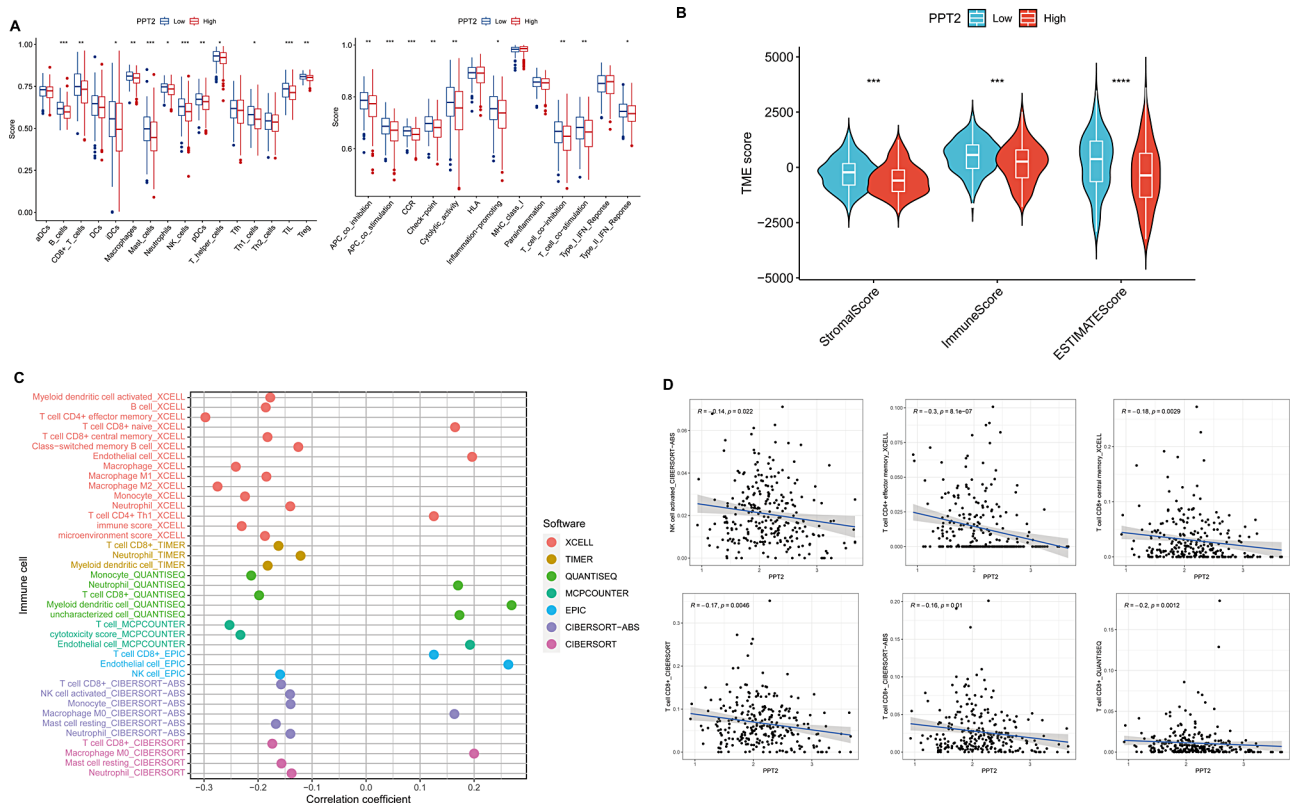


Fig. 7 Correlation of PPT2 expression with immune infiltration level in OC. **(A)** The abundance of different immune cells and immune pathways in the low and high expression of PPT2. **(B)** Comparison of tumor microenvironment (TME) scores between the low and high expression of PPT2. **(C)** Immune infiltration scores of different cells associated with PPT2 expression by different algorithms. **(D)** Correlation between the PPT2 expression and some representative immune infiltration cell scores. * $p < 0.05$, ** $p < 0.01$, and *** $p < 0.001$

multiple cohorts, including our in-house dataset, the TCGA dataset, and other GEO datasets. We also showed the pan-cancer survival correlation with the expression of PPT2, PPT2 showed a significant risky or protective role in many cancer types. Moreover, a multivariable survival model including the PPT2 expression showed that PPT2 could serve as an independent prognostic factor for OS and PFS. A clinical nomogram based on PPT2 expression combined with clinical factors was constructed to visually predict patient outcomes and accurately predict the survival of patients at 1, 3 and 5 years. Further in vitro experiments proved that PPT2 could inhibit the proliferation and metastasis of OC cells. The important implications of PPT2's involvement in prognosis prediction in OC deserved to be thoroughly explored in further experiments. We also found that a high expression level of PPT2 was closely related to the activation of HALLMARK EPITHELIAL MESENCHYMAL TRANSITION, HALLMARK IL6 JAK STAT3 SIGNALING, HALLMARK KRAS SIGNALING UP, the activation of these related pathways could promote tumorigenesis and development, we here postulated that within neoplastic

tissues, the diminished expression of gene PPT2 served to promote the pathways, subsequently facilitating the proliferation of cancerous cells, thus leading to adverse prognostic outcomes for the OC patients. Many hub genes were found to be closely related to cancer. VPS52 induced apoptosis via cathepsin D in gastric cancer [40]. RGL2 drove the metastatic progression of colorectal cancer [41]. SLC39A7 was a novel determinant of ferroptosis [42]. PFDN6 was a potential predictive marker of dexamethasone resistance in childhood acute lymphoblastic leukemia [43]. ZBTB9 was a novel biomarker in Liver Hepatocellular Carcinoma [44]. RING1 promoted the transformation of hepatic progenitor cells into cancer stem cells through the Wnt/ β -catenin signaling pathway [45].

In recent years, compared with the standard treatments (surgery, chemotherapy and radiotherapy), cancer immunotherapy seemed to significantly improve certain patients' clinical outcomes and quality of life [46]. The previous study showed that the intra-tumoral T cells were related to improved PFS and OS in patients with OC and were associated with the activation of antitumor

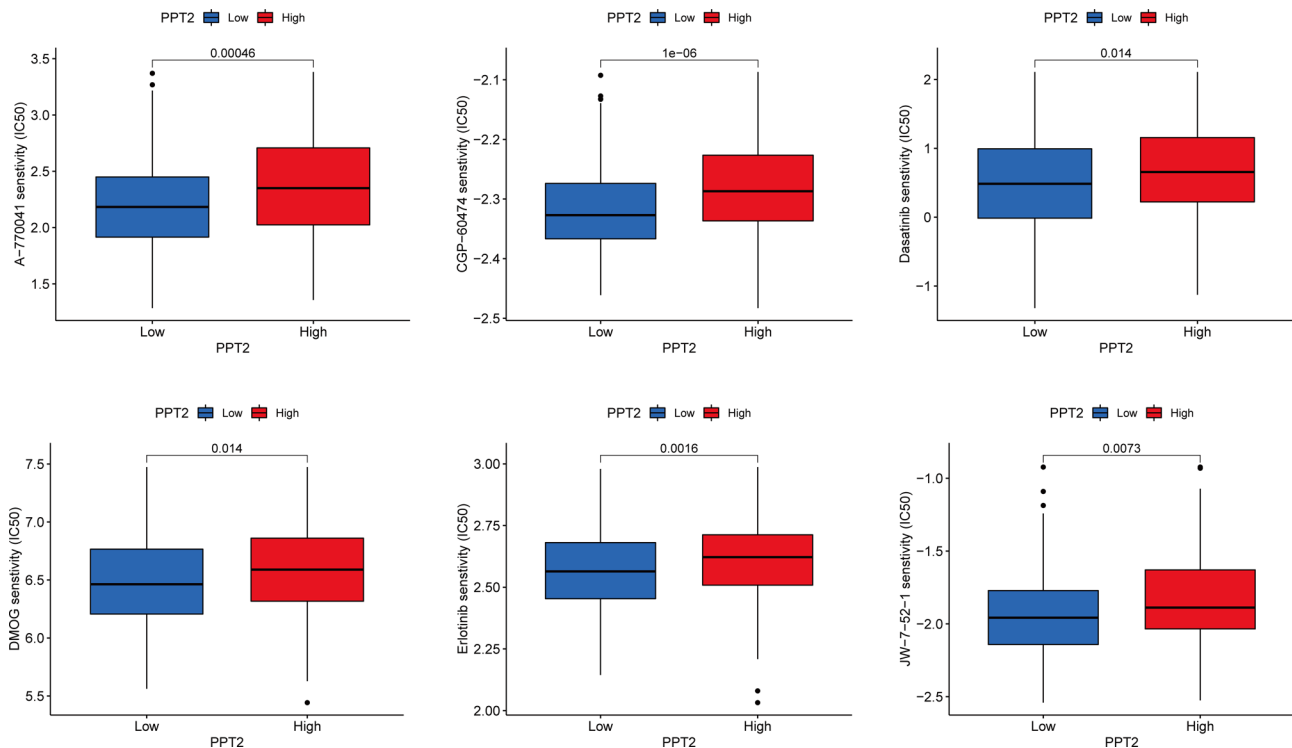


Fig. 8 Evaluation of sensitivity to chemotherapy for PPT2

mechanisms [47, 48]. Some studies described that the intraepithelial TILs were the relevant prognostic factors for the prognosis of OC patients [47, 49, 50]. However, effective strategies to identify OC patients who may benefit from immunotherapy were needed. In this study, it was confirmed that PPT2 expression was correlated with immune infiltration levels in OC. More immune cells, such as CD8+T cells and NK cells, were associated with lower PPT2 expression by different algorithms displayed in the immune cell bubble chart by different methods. Moreover, PPT2 was negatively correlated with an up-regulated immune score, stromal score, and estimate score. All the above results indicated that the PPT2 expression was significantly correlated with the immune infiltration status of patients. We also found that the IC50 values of the A-770,041, CGP-60,474, Dasatinib, DMOG, Erlotinib and JW-7-52-1 were lower in the low PPT2 group. Therefore, we proposed that administering immunotherapy and chemotherapy earlier could significantly improve clinical outcomes for patients with low PPT2 expression, who typically had poor prognoses. We speculated that the molecular mechanism of the lower expression level of PPT2 in OC may be related to the activation of tumor promotion pathways, such as HALLMARK EPITHELIAL MESENCHYMAL TRANSITION. In this study, compared to previous research on

PPT2 in ccRCC and oropharyngeal cancer, we conducted a more comprehensive investigation encompassing cellular functions, tumor tissue expression, survival analysis, immunological profiling, and pharmacological evaluation. The potential clinical implications of using PPT2 as a prognostic biomarker and its role in immunotherapy were significant. Our study, the first to report on PPT2 expression in OC, identified low PPT2 expression as a potentially unfavorable biomarker for OC patients, validated in an independent in-house cohort and multiple public datasets. We demonstrated that decreased PPT2 expression correlated with lower survival rates and found a negative correlation between PPT2 expression and immune cell infiltration. Additionally, patients with low PPT2 expression exhibited lower IC50 values for chemotherapeutic drugs, suggesting they might benefit more from immunotherapy and chemotherapy. Despite these promising findings, translating these results into clinical practice faced several challenges, including the need for prospective validation, addressing individual variability, and standardizing detection methods. Furthermore, the retrospective nature of our data analysis might introduce inherent biases, and selection biases in datasets could impact the generalizability of our conclusions. Future research should focus on conducting prospective studies with diverse cohorts, performing detailed mechanistic

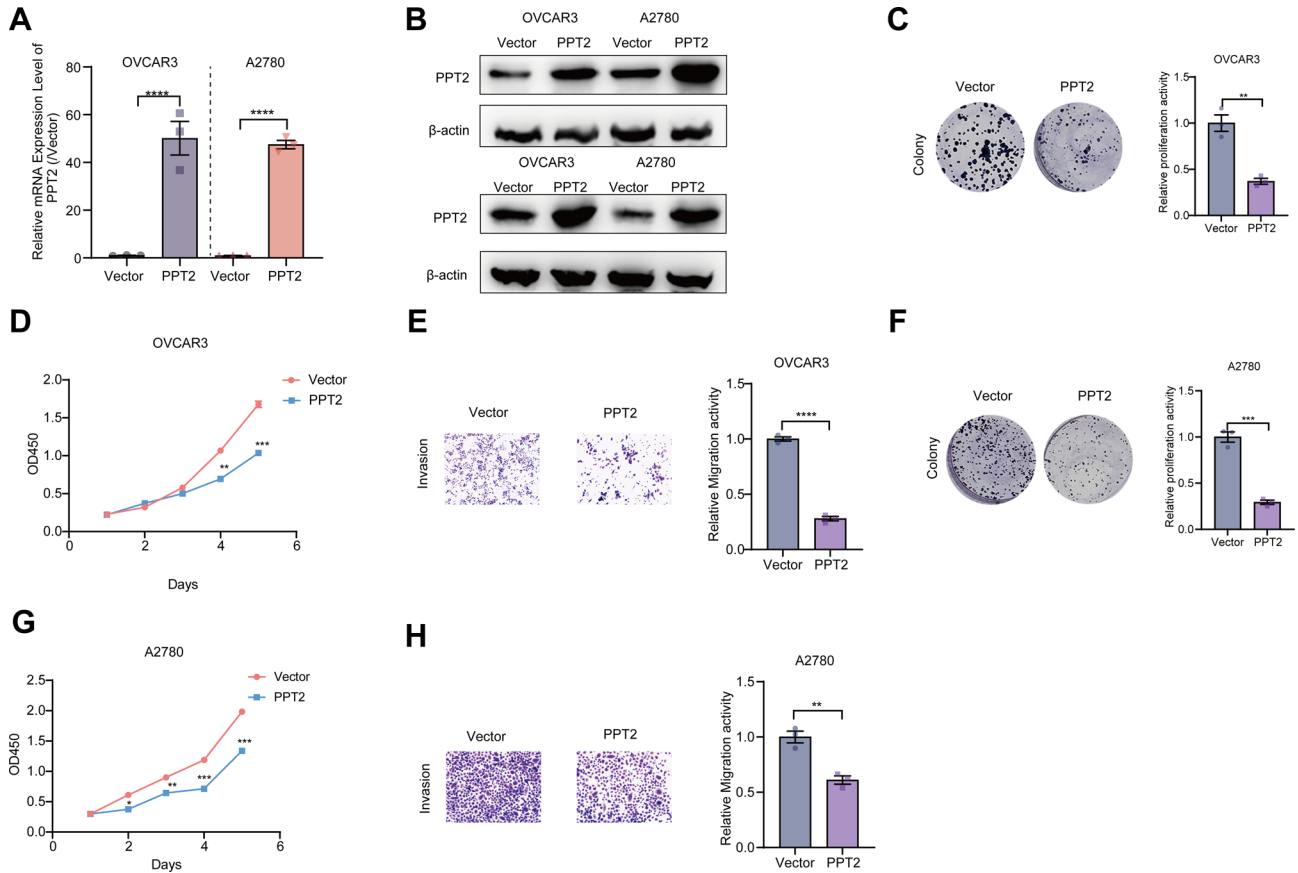


Fig. 9 PPT2 reduced proliferation and invasion of OC cells. **(A-B)** Stable overexpression of PPT2 in OVCAR3 and A2780 cells. The expression of PPT2 was verified at both mRNA and protein levels. **(C)** Overexpression of PPT2 impaired the colony-forming ability of OVCAR3 cells. **(D)** Overexpression of PPT2 significantly reduced the proliferation rate of OVCAR3 cells. **(E)** Transwell assay results showed that overexpression of PPT2 could significantly decreased the invasion of OVCAR3 cells. **(F)** Overexpression of PPT2 impaired the colony-forming ability of A2780 cells. **(G)** Overexpression of PPT2 significantly reduced the proliferation rate of A2780 cells. **(H)** Transwell assay results showed that overexpression of PPT2 could significantly decreased the invasion of A2780 cells. * $p < 0.05$, ** $p < 0.01$, and *** $p < 0.001$

studies to uncover the biological pathways involving PPT2, developing standardized detection methods, exploring integration with other biomarkers, and implementing longitudinal studies to monitor PPT2 expression over time. Addressing these challenges were crucial for

realizing the potential of PPT2 as a valuable clinical biomarker and therapeutic guide, as our findings suggested that PPT2 could serve as a favorable prognostic biomarker for OC and might play a critical role in predicting responses to immunotherapy and chemotherapy.

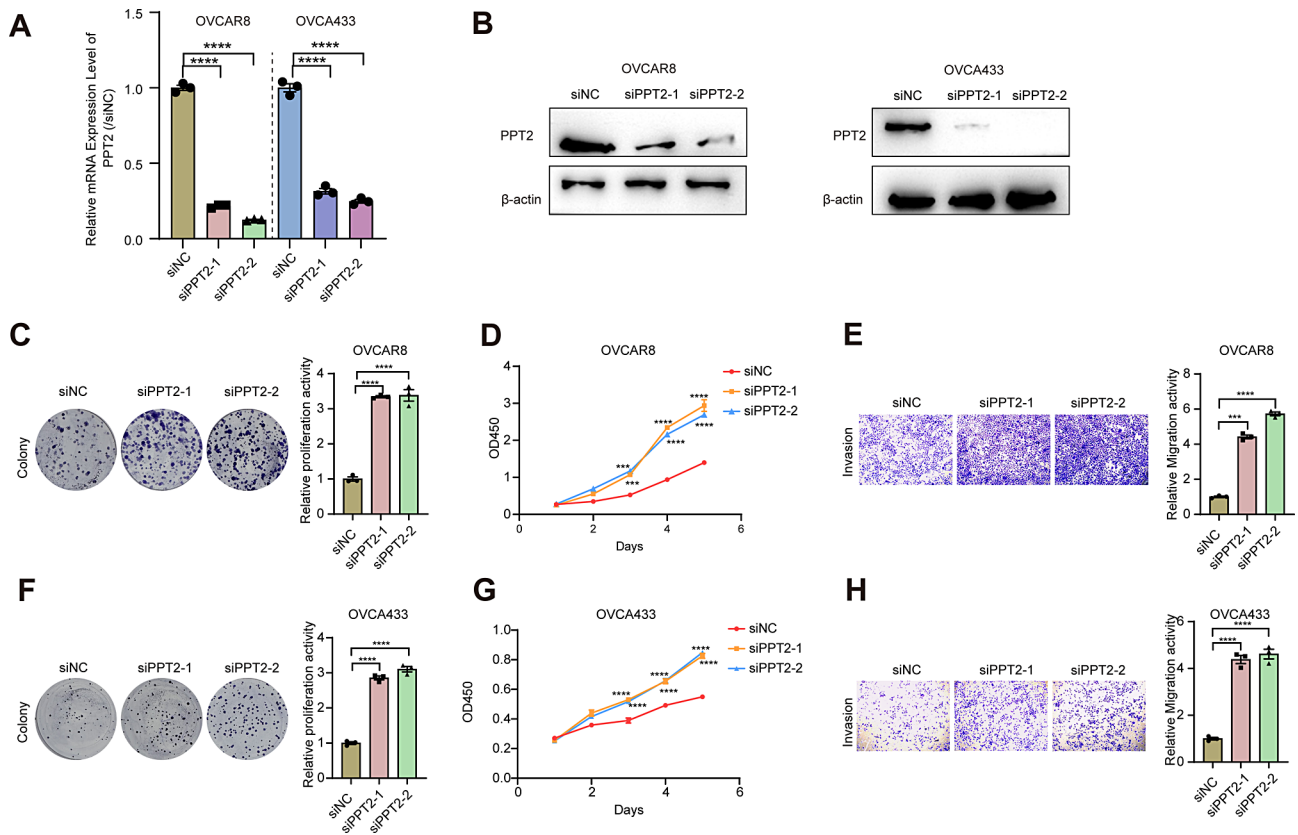


Fig. 10 PPT2 promoted proliferation and invasion of OC cells. **(A–B)** Decreased expression of PPT2 in OVCAR8 and OVCA433 cells. The expression of PPT2 was verified at both mRNA and protein levels. **(C)** Decreased expression of PPT2 promoted the colony-forming ability of OVCAR8 cells. **(D)** Decreased expression of PPT2 significantly promoted the proliferation rate of OVCAR8 cells. **(E)** Transwell assay results showed that decreased expression of PPT2 could significantly promoted the invasion of OVCAR8 cells. **(F)** Decreased expression of PPT2 promoted the colony-forming ability of OVCA433 cells. **(G)** Decreased expression of PPT2 significantly promoted the proliferation rate of OVCA433 cells. **(H)** Transwell assay results showed that decreased expression of PPT2 could significantly promoted the invasion of OVCA433 cells. * $p < 0.05$, ** $p < 0.01$, and *** $p < 0.001$

Conclusion

In conclusion, it was the first time that the clinical implications of PPT2 expression were reported in OC. The low expression of PPT2 was demonstrated to be a potentially unfavorable biomarker for OC patients in an independent in-house cohort and in multiple public datasets. A negative correlation between immune cells and PPT2 expression was found and lower IC50 values of drugs, implying that immunotherapy and chemotherapy might be more beneficial to patients with low PPT2 expression. However, the present findings required more further studies including prospective and multi-center studies.

Abbreviations

- ATCC American type culture collection
- AUC Area under the curve
- CCK-8 Cell counting kit-8
- ccRCC Clear cell renal cell carcinoma
- CESC Cervical cancer
- DLBC Lymphoid neoplasm diffuse large b-cell lymphoma
- DSS Disease-free survival
- EMT Epithelial-to-mesenchymal transition
- FIGO International federation of gynecology and obstetrics
- GBM Glioblastoma multiforme

- GDSC Genomics of drug sensitivity in cancer
- GEO Gene expression omnibus
- GTEx Genotype-tissue expression
- IC50 Half-maximal inhibitory concentration
- IHC Immunohistochemistry
- INCL Infantile neural ceroid lipofuscinosis
- KICH Kidney chromophobe
- LUAD Lung adenocarcinoma
- OC Ovarian cancer
- OS Overall survival
- PAAD Pancreatic adenocarcinoma
- PARP Poly-ADP ribose polymerase
- PCR Polymerase chain reaction
- PPI Protein-protein interaction
- PPT Palmitoyl protein thioesterase
- PPT1 Palmitoyl protein thioesterase 1
- PPT2 Palmitoyl protein thioesterase 2
- PFS Progression-free survival
- RT-qPCR Real time-quantitative polymerase chain reaction
- SRT Short tandem repeat
- TCGA The cancer genome atlas
- ThCA Thyroid carcinoma
- ThYM Thymoma
- TIL Tumor-infiltrating lymphocytes
- TISCH2 Tumor immune single-cell hub 2

Supplementary Information

The online version contains supplementary material available at <https://doi.org/10.1186/s13048-024-01527-9>.

Supplementary Material 1

Supplementary Material 2

Acknowledgements

We acknowledge the contribution of all members who helped in this study.

Author contributions

All authors contributed to the study's conception and design. Material preparation, data collection, and analysis were performed by Hui Xu, Yan Zhang, Zhen Xie, Xiao-feng Xie, Wen-lan Qiao, Miao Wang, Bei-bei Zhao. The first draft of the manuscript was written by Tian Hua, Hui Xu. All authors read and approved the final manuscript.

Funding

No fund.

Data availability

No datasets were generated or analysed during the current study.

Declarations

Ethics approval and consent to participate

The Affiliated Xingtai People Hospital of Hebei Medical University Ethics Committee reviewed and approved our study (2018 [07]). Written informed consent was provided by all patients. This study was performed in line with the principles of the Declaration of Helsinki.

Consent for publication

Written informed consents were obtained from all enrolled patients.

Clinical trial number

Not applicable.

Competing interests

The authors declare no competing interests.

Received: 16 July 2024 / Accepted: 1 October 2024

Published online: 11 October 2024

References

- Siegel RL, Miller KD, Jemal A. Cancer statistics, 2020. *CA Cancer J Clin*. 2020;70(1):7–30.
- Sung H, Ferlay J, Siegel RL, Laversanne M, Soerjomataram I, Jemal A, et al. Global Cancer statistics 2020: GLOBOCAN estimates of incidence and Mortality Worldwide for 36 cancers in 185 countries. *CA Cancer J Clin*. 2021;71(3):209–49.
- Yang H, Pawitan Y, Fang F, Czene K, Ye W. Biomarkers and Disease trajectories Influencing women's Health: results from the UK Biobank Cohort. *Phenomics*. 2022;2(3):184–93.
- Prat J. FIGO's staging classification for cancer of the ovary, fallopian tube, and peritoneum: abridged republication. *J Gynecol Oncol*. 2015;26(2):87–9.
- Katsumata N, Yasuda M, Isonishi S, Takahashi F, Michimae H, Kimura E, et al. Long-term results of dose-dense paclitaxel and carboplatin versus conventional paclitaxel and carboplatin for treatment of advanced epithelial ovarian, fallopian tube, or primary peritoneal cancer (JGOG 3016): a randomised, controlled, open-label trial. *Lancet Oncol*. 2013;14(10):1020–6.
- Mirza MR, Coleman RL, González-Martín A, Moore KN, Colombo N, Ray-Coquard I, et al. The forefront of ovarian cancer therapy: update on PARP inhibitors. *Ann Oncol*. 2020;31(9):1148–59.
- Lehtovirta M, Kyttilä A, Eskelinen EL, Hess M, Heinonen O, Jalanko A. Palmitoyl protein thioesterase (PPT) localizes into synaptosomes and synaptic vesicles in neurons: implications for infantile neuronal ceroid lipofuscinosis (INCL). *Hum Mol Genet*. 2001;10(1):69–75.
- Gupta P, Soyombo AA, Atashband A, Wisniewski KE, Shelton JM, Richardson JA, et al. Disruption of PPT1 or PPT2 causes neuronal ceroid lipofuscinosis in knockout mice. *Proc Natl Acad Sci U S A*. 2001;98(24):13566–71.
- Lu JY, Hofmann SL. Inefficient cleavage of palmitoyl-protein thioesterase (PPT) substrates by aminothiols: implications for treatment of infantile neuronal ceroid lipofuscinosis. *J Inherit Metab Dis*. 2006;29(1):119–26.
- Rebecca VW, Nicastrì MC, Fennelly C, Chude CI, Barber-Rotenberg JS, Ronghe A, et al. PPT1 promotes Tumor Growth and is the molecular target of chloroquine derivatives in Cancer. *Cancer Discov*. 2019;9(2):220–9.
- Xu J, Su Z, Cheng X, Hu S, Wang W, Zou T, et al. High PPT1 expression predicts poor clinical outcome and PPT1 inhibitor DC661 enhances sorafenib sensitivity in hepatocellular carcinoma. *Cancer Cell Int*. 2022;22(1):115.
- Yuan C, Xiong Z, Shi J, Peng J, Meng X, Wang C, et al. Overexpression of PPT2 represses the clear cell renal cell carcinoma progression by reducing epithelial-to-mesenchymal transition. *J Cancer*. 2020;11(5):1151–61.
- Yang H, Xu F, Xiao K, Chen Y, Tian Z. N-Glycoproteomics study of putative N-Glycoprotein biomarkers of Drug Resistance in MCF-7/ADR cells. *Phenomics*. 2021;1(6):269–84.
- Goldman MJ, Craft B, Hastie M, Repečka K, McDade F, Kamath A, et al. Visualizing and interpreting cancer genomics data via the Xena platform. *Nat Biotechnol*. 2020;38(6):675–8.
- Wang S, Xiong Y, Zhao L, Gu K, Li Y, Zhao F, et al. UCSCXenaShiny: an R/CRAN package for interactive analysis of UCSC Xena data. *Bioinformatics*. 2022;38(2):527–9.
- Yu G, Wang LG, Han Y, He QY. clusterProfiler: an R package for comparing biological themes among gene clusters. *Omics*. 2012;16(5):284–7.
- Xu S, Hu E, Cai Y, Xie Z, Luo X, Zhan L, et al. Using clusterProfiler to characterize multiomics data. *Nat Protoc*. 2024;1–29.
- Yoshihara K, Shahmoradgoli M, Martínez E, Vegesna R, Kim H, Torres-García W, et al. Inferring tumour purity and stromal and immune cell admixture from expression data. *Nat Commun*. 2013;4:2612.
- Li T, Fu J, Zeng Z, David C, Li J, Chen Q, et al. TIMER2.0 for analysis of tumor-infiltrating immune cells. *Nucleic Acids Res*. 2020;48(W1):W509–14.
- Geeleher P, Cox NJ, Huang R. Clinical drug response can be predicted using baseline gene expression levels and in vitro drug sensitivity in cell lines. *Genome Biology*. 2014;15(3):R47.
- Geeleher P, Cox N, Huang RS. pRRophetic: an R package for prediction of clinical chemotherapeutic response from tumor gene expression levels. *PLoS ONE*. 2014;9(9):e107468.
- Vasaikar SV, Straub P, Wang J, Zhang B. LinkedOmics: analyzing multi-omics data within and across 32 cancer types. *Nucleic Acids Res*. 2018;46(D1):D956–63.
- Cook H, Doncheva N, Szklarczyk D, Mering CV, Jensen L. Viruses.STRING: a virus-host protein-protein Interaction Database. *Viruses*. 2018;10(10).
- Shannon P, Cytoscape. A Software Environment for Integrated Models of Biomolecular Interaction Networks. *Genome Res*. 2003;13(11):2498–504.
- Lin DT, Conibear E. Enzymatic protein depalmitoylation by acyl protein thioesterases. *Biochem Soc Trans*. 2015;43(2):193–8.
- Calero G, Gupta P, Nonato MC, Tandel S, Biehl ER, Hofmann SL, et al. The crystal structure of palmitoyl protein thioesterase-2 (PPT2) reveals the basis for divergent substrate specificities of the two lysosomal thioesterases, PPT1 and PPT2. *J Biol Chem*. 2003;278(39):37957–64.
- Brun S, Bestion E, Raymond E, Bassissi F, Jilkova ZM, Mezouar S, et al. GNS561, a clinical-stage PPT1 inhibitor, is efficient against hepatocellular carcinoma via modulation of lysosomal functions. *Autophagy*. 2022;18(3):678–94.
- Harding JJ, Awada A, Roth G, Decaens T, Merle P, Kotecki N, et al. First-In-Human effects of PPT1 inhibition using the oral treatment with GNS561/Ezurpimtrostat in patients with primary and secondary liver cancers. *Liver Cancer*. 2022;11(3):268–77.
- Vergoten G, Bailly C. Binding of hydroxychloroquine and chloroquine dimers to palmitoyl-protein thioesterase 1 (PPT1) and its glycosylated forms: a computational approach. *J Biomol Struct Dyn*. 2022;40(18):8197–205.
- Tian W, Li C, Ren J, Li P, Zhao J, Li S et al. Identification of PPT1 as a lysosomal core gene with prognostic value in hepatocellular carcinoma. *Biosci Rep*. 2023;43(5).
- Luo Q, Li X, Gan G, Yang M, Chen X, Chen F. PPT1 reduction contributes to Erianin-Induced growth inhibition in oral squamous carcinoma cells. *Front Cell Dev Biol*. 2021;9:764263.

32. Sharma G, Ojha R, Noguera-Ortega E, Rebecca VW, Attanasio J, Liu S et al. PPT1 inhibition enhances the antitumor activity of anti-PD-1 antibody in melanoma. *JCI Insight*. 2020;5(17).
33. Bestion E, Rachid M, Tijeras-Raballand A, Roth G, Decaens T, Ansaldo C, et al. Ezurpimtrostat, a palmitoyl-protein Thioesterase-1 inhibitor, combined with PD-1 inhibition provides CD8(+) lymphocyte repopulation in Hepatocellular Carcinoma. *Target Oncol*. 2024;19(1):95–106.
34. Sales Conniff A, Singh J, Heller R, Heller LC. Pulsed Electric Fields Induce STING Palmitoylation and polymerization independently of plasmid DNA Electrotransfer. *Pharmaceutics*. 2024;16(3).
35. Meng LN, Liu JY, Wang YT, Ni SS, Xiang MJ. The discovery of potential phosphopantetheinyl transferase Ppt2 inhibitors against drug-resistant *Candida albicans*. *Braz J Microbiol*. 2020;51(4):1665–72.
36. Dobb KS, Kaye SJ, Beckmann N, Thain JL, Stateva L, Birch M, et al. Characterisation of the *Candida albicans* Phosphopantetheinyl Transferase Ppt2 as a potential Antifungal Drug Target. *PLoS ONE*. 2015;10(11):e0143770.
37. Gupta P, Soyombo AA, Shelton JM, Wilkofsky IG, Wisniewski KE, Richardson JA, et al. Disruption of PPT2 in mice causes an unusual lysosomal storage disorder with neurovisceral features. *Proc Natl Acad Sci U S A*. 2003;100(21):12325–30.
38. Langdon R, Richmond R, Elliott HR, Dudding T, Kazmi N, Penfold C, et al. Identifying epigenetic biomarkers of established prognostic factors and survival in a clinical cohort of individuals with oropharyngeal cancer. *Clin Epigenetics*. 2020;12(1):95.
39. Soyombo AA, Hofmann SL. Molecular cloning and expression of palmitoyl-protein thioesterase 2 (PPT2), a homolog of lysosomal palmitoyl-protein thioesterase with a distinct substrate specificity. *J Biol Chem*. 1997;272(43):27456–63.
40. Zhang J, Lin Y, Hu X, Wu Z, Guo W. VPS52 induces apoptosis via cathepsin D in gastric cancer. *J Mol Med (Berl)*. 2017;95(10):1107–16.
41. Sun MS, Yuan LT, Kuei CH, Lin HY, Chen YL, Chiu HW et al. RGL2 drives the metastatic progression of Colorectal Cancer via preventing the protein degradation of β -Catenin and KRAS. *Cancers (Basel)*. 2021;13(8).
42. Chen PH, Wu J, Xu Y, Ding CC, Mestre AA, Lin CC, et al. Zinc transporter ZIP7 is a novel determinant of ferroptosis. *Cell Death Dis*. 2021;12(2):198.
43. Dehghan-Nayeri N, Rezaei-Tavirani M, Omrani MD, Gharehbaghian A, Goudarzi Pour K, Eshghi P. Identification of potential predictive markers of dexamethasone resistance in childhood acute lymphoblastic leukemia. *J Cell Commun Signal*. 2017;11(2):137–45.
44. Zhang Z, Wu L, Li J, Chen J, Yu Q, Yao H, et al. Identification of ZBTB9 as a potential therapeutic target against dysregulation of tumor cells proliferation and a novel biomarker in Liver Hepatocellular Carcinoma. *J Transl Med*. 2022;20(1):602.
45. Zhu K, Li J, Li J, Sun J, Guo Y, Tian H, et al. Ring1 promotes the transformation of hepatic progenitor cells into cancer stem cells through the Wnt/ β -catenin signaling pathway. *J Cell Biochem*. 2020;121(8–9):3941–51.
46. DeBerardinis RJ. Tumor Microenvironment, Metabolism, and Immunotherapy. *N Engl J Med*. 2020;382(9):869–71.
47. Wang Q, Lou W, Di W, Wu X. Prognostic value of tumor PD-L1 expression combined with CD8(+) tumor infiltrating lymphocytes in high grade serous ovarian cancer. *Int Immunopharmacol*. 2017;52:7–14.
48. Zhang L, Conejo-Garcia JR, Katsaros D, Gimotty PA, Massobrio M, Regnani G, et al. Intratumoral T cells, recurrence, and survival in epithelial ovarian cancer. *N Engl J Med*. 2003;348(3):203–13.
49. Fanale D, Dimino A, Pedone E, Brando C, Corsini LR, Filorizzo C et al. Prognostic and predictive role of Tumor-infiltrating lymphocytes (TILs) in Ovarian Cancer. *Cancers (Basel)*. 2022;14(18).
50. Hamanishi J, Mandai M, Iwasaki M, Okazaki T, Tanaka Y, Yamaguchi K, et al. Programmed cell death 1 ligand 1 and tumor-infiltrating CD8+ T lymphocytes are prognostic factors of human ovarian cancer. *Proc Natl Acad Sci U S A*. 2007;104(9):3360–5.

Publisher's note

Springer Nature remains neutral with regard to jurisdictional claims in published maps and institutional affiliations.